J|A|C|S
ARTICLES
Published on Web 09/08/2005

# Low-Temperature Studies of Encapsulated Proteins

Wade D. Van Horn, Alana K. Simorellis, and Peter F. Flynn*

*Contribution from the Department of Chemistry, University of Utah, Salt Lake City, Utah 84112-0850*

Received April 29, 2005; E-mail: pfflynn@chem.utah.edu

***Abstract:*** Water-soluble proteins encapsulated within reverse micelles may be studied under a variety of conditions, including low temperature and a wide range of buffer conditions. Direct high-resolution detection of information relating to protein folding intermediates and pathways can be monitored by low-temperature solution NMR. Ubiquitin encapsulated within AOT reverse micelles was studied using multidimensional multinuclear solution NMR to determine the relationship between protein structure, temperature, and ionic strength. Ubiquitin resonances were monitored by $^{15}$N HSQC NMR experiments at varying temperatures and salt concentrations. Our results indicate that the structure of the encapsulated protein at low temperature experiences perturbation arising from two major influences, which are reverse micelle−protein interactions and low-temperature effects (e.g., cold denaturation). These two effects are impossible to distinguish under conditions of low ionic strength. Elevated concentrations of nondenaturing salt solutions defeat the effects of reverse micelle−protein interactions and reveal low-temperature protein unfolding. High ionic strength shielding stabilizes the reverse micelle at low temperatures, which reduces the electrostatic interaction between the protein and reverse micelle surfaces, allowing the phenomenon of cold denaturation to be explored.

## Introduction

Reverse micelles are stable surfactant aggregates that spontaneously form around an aqueous core. AOT (also Aerosol-OT, dioctyl sulfosuccinate, or bis(2-ethylhexyl)sodium sulfosuccinate), the most common reverse micelle forming surfactant, forms stable reverse micelles in apolar solvents. Reverse micelle assemblies can be tuned to accommodate a wide range of host molecules by varying the water loading ($w_0 = [H_2O]/[\text{surfactant}]$), salt, buffer, and pH (Figure 1). The process of host molecule accommodation is called encapsulation, and many proteins of various size and surface charge density have been encapsulated in AOT reverse micelles.[1−7] Ubiquitin is the protein standard for reverse micellar encapsulation because the protein is highly stable, readily encapsulated, biologically relevant, and has been shown to adopt native structure in the encapsulated state.[8] The completeness with which ubiquitin has been examined by both structural and biophysical methods makes it an excellent target for cold denaturation studies.

Reverse micelles are of particular interest in biophysics because of their ability to confine host molecules to small volumes with direct control of the environment, and support studies of host molecules under a wide range of conditions.[9] The two specific conditions probed in the current investigation are protein confinement and the influence of low temperature on protein structure. The data presented here demonstrate that crowding and low-temperature effects (e.g., reverse micelle−protein interactions and cold denaturation) can be tuned, providing additional control over the encapsulated environment.

Low-temperature studies in reverse micelles are possible because the nanodispersion is stable in nonaqueous, low-polarity solvents, which freeze at temperatures much below the freezing point of water.[10] Pentane is commonly used as the solvent in encapsulated protein studies, with a freezing point of −130 °C, which is well below the freezing point of bulk water and the predicted cold denaturation temperature of proteins.[11] Reverse micelle protein encapsulation at low temperatures thus promises to provide a general and effective platform for studies of protein cold denaturation.

Cold denaturation is the process of low-temperature protein unfolding, which arises because the free energy of protein unfolding ($\Delta G_{D-N}$) between native and denatured states has a convex dependence on temperature:[11,12]

$$\Delta G_{D-N(T2)} = \Delta H_{D-N(T1)} + \Delta C_p(T_2 - T_1) - T_2(\Delta S_{D-N(T1)} + \Delta C_p \ln(\{T_2\}/\{T_1\}))$$

The maximum value of $\Delta G_{D-N}$ for most proteins occurs near room temperature, and because proteins generally have large

(1) Andrade, S. M.; Carvalho, T. I.; Viseu, M. I.; Costa, S. M. B. *Eur. J. Biochem.* **2004**, *271*, 734−744.
(2) Rariy, R. V.; Bec, N.; Saldana, J.-L.; Nametkin, S. N.; Mozhaev, V. V.; Klyachko, N. L.; Levashov, A. V.; Balny, C. *FEBS Lett.* **1995**, *364*, 98−100.
(3) Meloa, E. P.; Costa, S. ı. M. B.; Cabral, J. M. S.; Fojan, P.; Petersen, S. B. *Chem. Phys. Lipids* **2003**, *124*, 37−47.
(4) Anarbaev, R. O.; Elepov, I. B.; Lavrik, O. I. *Biochim. Biophys. Acta* **1998**, *1384*, 315−324.
(5) Salom, D.; Abad, C.; Braco, L. *Biochemistry* **1992**, *31*, 8072−8079.
(6) Gerhardt, N. I.; Dungan, S. R. *Biotechnol. Bioeng.* **2002**, *78*, 60−72.
(7) Klyachko, N. L.; Levashov, P. A.; Levashov, A. V.; Balny, C. *Biochem. Biophys. Res.* **1999**, *254*, 685−688.
(8) Babu, C. R.; Flynn, P. F.; Wand, A. J. *J. Am. Chem. Soc.* **2001**, *123*, 2691−2692.
(9) Peterson, R. W.; Anabalagan, K.; Tommos, C.; Wand, A. J. *J. Am. Chem. Soc.* **2004**, *126*, 9498−9499.
(10) Wand, A. J.; Babu, C. R.; Flynn, P. F.; Milton, M. J. In *Protein NMR for the Millennium*; Berliner, L. J., Ed.; Kluwer Academic/Plenum Publishers: New York, 2003; pp 121−160.

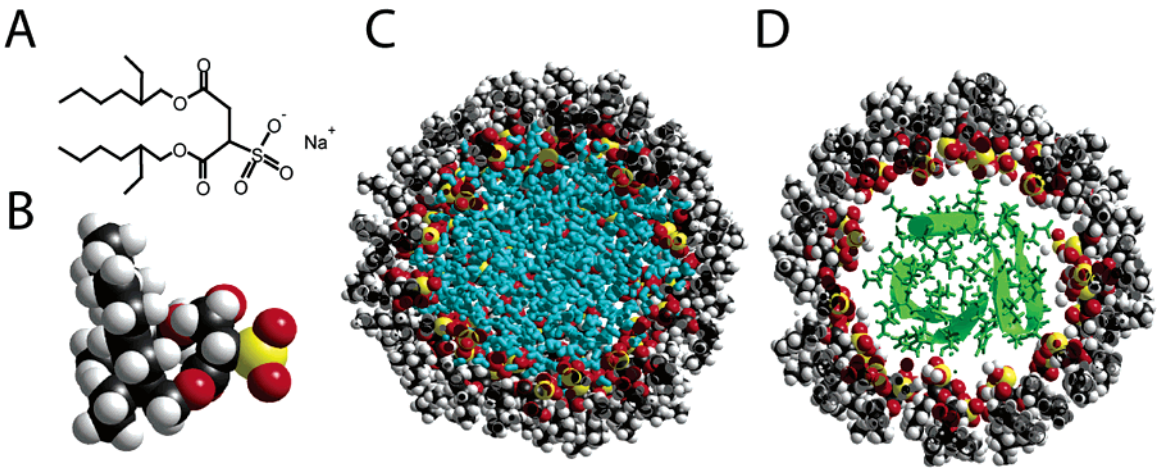


***Figure 1.*** Reverse micelle models. (A) Vector diagram of AOT or dioctyl sulfosuccinate. AOT is the most commonly used reverse micelle forming surfactant. (B) Space filling energy minimized model of AOT. The protons are white, carbons are black, oxygens are red, and sulfur is yellow. The inherent wedge shape of AOT allows this surfactant to be a facile reverse micelle former. AOT molecules come together to form a reverse micelle, which is an aggregation of surfactants surrounding a polar, charged core (usually an aqueous core). (C) Cut-away diagram of a reverse micelle model with the same color designations as (B), except that the cyan designates water molecules. This reverse micelle model is atomistically explicit and energy minimized. The model assumes an aggregation number of 75 surfactants, with corresponding $Na^+$ counterions, and a neat water core of 750 $H_2O$ molecules (e.g., a $w_0$ of 10). (D) Diagram of a cut-away reverse micelle/protein ternary system where the green is ubiquitin. The diagram has the protein ubiquitin docked in the model from part C. This model shows the accurate relative sizes of ubiquitin to an AOT reverse micelle for a low $w_0$ micelle (e.g., $<5$ $w_0$ units).

heat capacities ($\Delta C_p$), protein destabilization occurs as the temperature varies from room temperature in either direction.[13] At the cold denaturation temperature, the free energy of protein unfolding becomes negative, and the protein unfolds. The cold denaturation temperature of most proteins is predicted to occur well below the freezing point of water, which poses significant challenges to the characterization of this phenomenon. The lower stability of proteins at cold temperatures is usually ascribed to increased solubility of hydrophobic residues in aqueous solutions at low temperature; for example, the stabilizing influence of the hydrophobic effect is reduced.[11,12]

Solution NMR spectroscopy is rapidly becoming the method of choice in studies of complex (ternary and quaternary) reverse micelle systems. NMR excels for reverse micelle studies because the method is readily applied and provides a direct measure of the water content and reverse micelle size. The water loading, $w_0$ (defined as the molar ratio of water to surfactant), can be directly measured by relatively straightforward $^1$H 1D experiments, an important element of experimental design that has been underappreciated historically in reverse micelle studies. The translational diffusion coefficient of the reverse micelle can be measured using pulsed field gradient diffusion NMR experiments, which provides an accurate measurement of the particle radius.[14] The structure of host molecules (e.g., encapsulated protein) can likewise be directly monitored using isotopically filtered NMR experiments, such as the $^{15}$N HSQC.[15] Finally, a high-resolution encapsulated protein structure was recently solved by NMR techniques, demonstrating the compatibility of encapsulation and standard structural methods.[8]

## Materials and Methods

**Protein Preparation and Purification.** The plasmid cw-ubq encoding human ubiquitin was transformed into chemically competent BL21 (DE3) expression cells (Invitrogen Corp.; Carlsbad, CA). Transformants were selected by ampicillin resistance and cultured at 37 °C on M9 minimal media, with the sole nitrogen source being $^{15}NH_4Cl$. The growth was monitored at 600 nm. At an optical density ($OD_{600}$) of 0.6, the cells were induced to overexpress $^{15}$N-labeled human ubiquitin with 0.5 mM IPTG. The culture was grown for 4 additional hours (terminal $OD_{600}$ ~1.3). Cells were harvested by centrifugation at 5000 rpm for 15 min at 4 °C, and then stored at −80 °C. The cells were thawed and incubated for 30 min in Ni-binding buffer (500 mM NaCl, 20 mM sodium phosphate, pH 7.4) containing lysozyme and 1 mM PMSF. The cell extract was then sonicated and cleared by centrifugation at 15 000 rpm for 1 h at 4 °C. The cell extract supernatant was cold filtered through a 0.45 $\mu$m filter (Pall Corp.; East Hills, NY). The extract containing C-terminal 6× His-tagged ubiquitin was affinity purified by a Ni-IDA column (Amersham Biosciences; Piscataway, NJ). The ubiquitin containing elutant was concentrated, and the buffer was exchanged by a stirred cell (Millipore; Billerica, MA) into 150 mM NaCl, 50 mM sodium phosphate, pH = 7.2, and then further purified by gel filtration chromatography (HiPrep 16/60 Sephacryl S-100 HR, Amersham Biosciences; Piscataway, NJ). The resulting ubiquitin solution was then concentrated and exchanged into $ddH_2O$ (>18 MΩ using the Biocel by Millipore; Billerica, MA) as above. After exchange into $ddH_2O$, the ubiquitin solution was aliquoted into 5 mg quantities and lyophilized. The yield of the protein following purification was approximately 20−30 mg pure protein per liter of cell culture.

**Reverse Micelle Sample Preparation.** AOT was purchased from Sigma-Aldrich and used without further purification. Approximately 0.029 g of AOT (Sigma-Aldrich Corp.; St. Louis, MO) and 650 $\mu$L of perdeuterated pentane (Cambridge Isotope Laboratories Inc.; Andover, MA) were added to a screw-cap NMR tube (Wilmad LabGlass; Buena, NJ) to make a 100 mM AOT solution. $^{15}$N isotopically enriched ubiquitin (5 mg) was hydrated in 23.4 $\mu$L or 46.9 $\mu$L ($w_0$ = 20 or 40) of either $ddH_2O$ or the appropriate buffer. The protein solution was added to the 100 mM AOT solution and shaken vigorously for 10 min. Four separate reverse micelle samples were prepared in parallel with the exception of varying ionic strength and water loading adjustments to maximize ubiquitin encapsulation. Three buffered, salt containing samples were generated using 50 mM NaOAc, pH 5.0, and 0.25, 1.0, and 1.5 M NaCl, respectively. The NaOAc buffer was prepared with and pH adjusted with HCl. The unbuffered sample was made with $ddH_2O$. All reverse micelle samples reconstituted with ionic surfactants,

(11) Fersht, A. *Structure and Mechanism in Protein Science A Guide to Enzyme Catalysis and Protein Folding*, 2nd ed.; W. H. Freeman and Company: New York, 1999; pp 511−512.
(12) Privalov, P. L. *Crit. Rev. Biochem. Mol. Biol.* **1990**, *25*, 281−305.
(13) Caldarelli, G.; De Los Rios, P. *J. Biol. Phys.* **2001**, *27*, 229−241.
(14) Simorellis, A. K.; Flynn, P. F. *J. Magn. Reson.* **2004**, *170*, 322−328.
(15) Flynn, P. F. *Prog. Nucl. Magn. Reson. Spectrosc.* **2004**, *45*, 31−51.

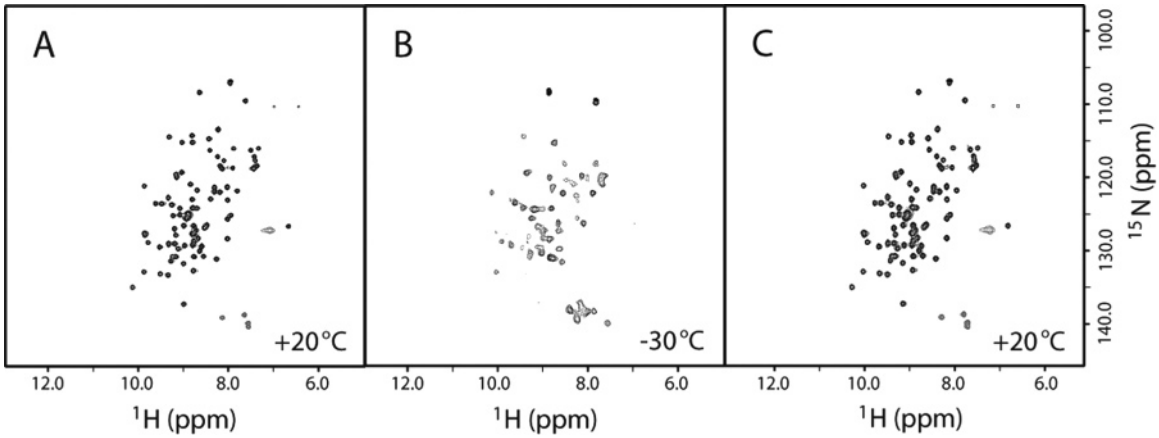


***Figure 2.*** Reversibility of low-temperature effects on ubiquitin monitored with $^{15}$N HSQC experiments. This panel of HSQC experiments shows that the changes in chemical shifts and/or disappearance of resonances are reversible. The sample is ubiquitin in 1 M NaCl, 50 mM NaOAc, pH 5.0 buffer, and 100 mM AOT. Panels A, B, and C are at +20, −30, and +20 °C, respectively. All spectra are recorded and processed identically.

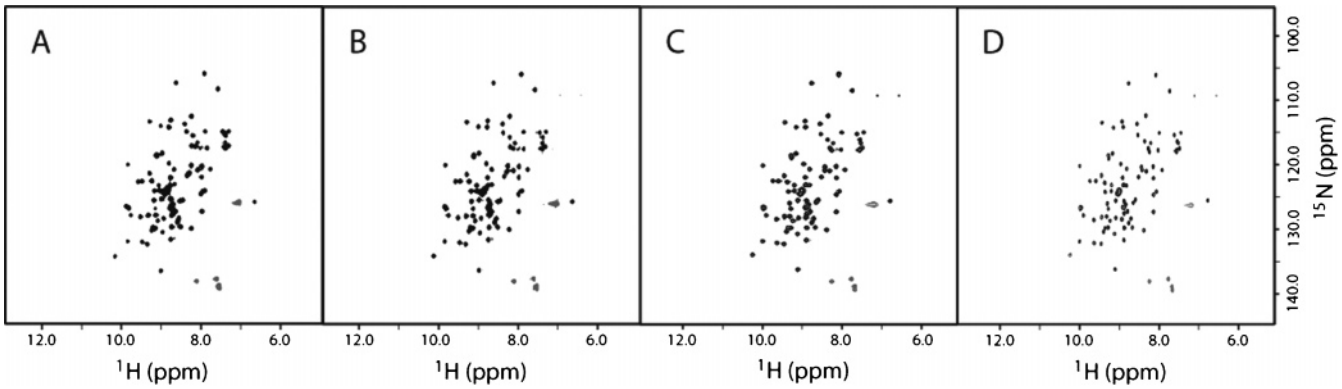


***Figure 3.*** The effects of increasing ionic strength on the structure of ubiquitin are negligible. All spectra are HSQC experiments at +20 °C of $^{15}$N-labeled ubiquitin in 100 mM AOT, 50 mM NaOAc, pH 5.0. The ionic strength is varied; (A), (B), (C), and (D) have no salt (e.g., dd$H_2O$), 0.25, 1.0, and 1.5 M NaCl, respectively. Spectra A, B, and C show constant intensities of the amide-proton correlations, while (D) shows decreased intensities. The decrease of intensity of (D) is a result of lower encapsulation efficiency as the salt concentration increases. All spectra are recorded and processed identically.

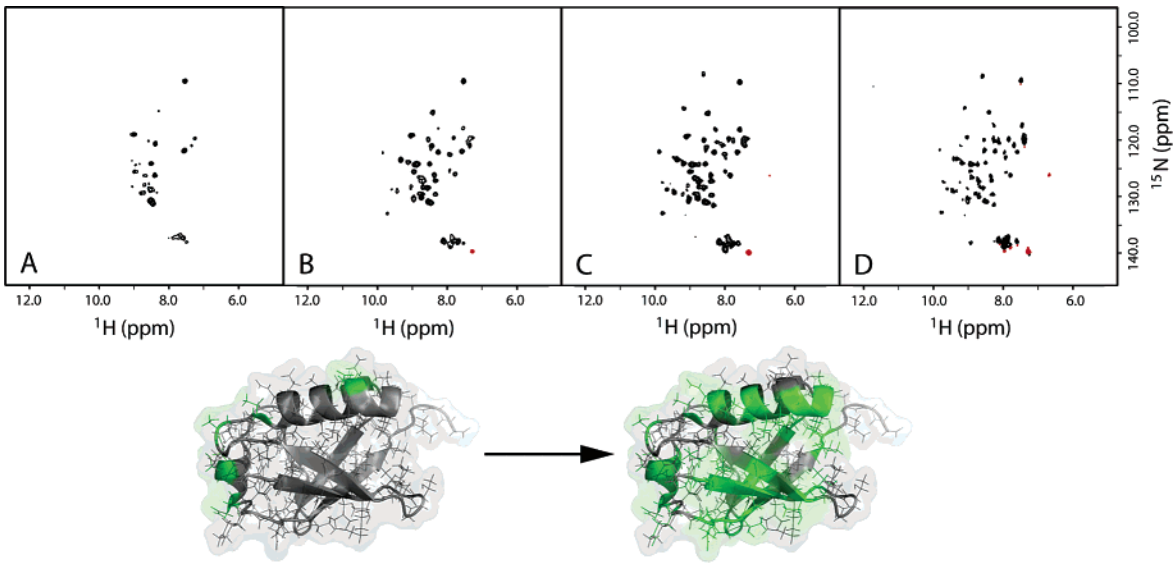


***Figure 4.*** The effects of low temperature are compensated by high ionic strength. All spectra are HSQC experiments at −30 °C of $^{15}$N-labeled ubiquitin in 100 mM AOT, 50 mM NaOAc, pH 5.0. The ionic strength is varied; (A), (B), (C), and (D) have no salt (e.g., neat water), 0.25, 1.0, and 1.5 M NaCl, respectively. Note that all spectra are recorded and processed identically. Observed amide proton and nitrogen correlations from spectra A and D are mapped onto a structural model of ubiquitin and highlighted in green.

such as AOT, have high constitutive ionic strengths because of high counterion concentrations; for example, the water pool within an AOT reverse micelle is >2 M in $Na^+$ ions. To maximize ubiquitin encapsulation efficiency, the samples containing $H_2O$ and 0.25 M NaCl were prepared with a target $w_0$ of 20, whereas at the high ionic strength, samples (1 and 1.5 M NaCl) would not encapsulate ubiquitin efficiently unless higher water loading values were used. The targeted water loadings of the high ionic strength samples were 40. Protein encapsula-

tion efficiency tends to decrease both with high ionic strength and also with very low water loadings ($w_0 < 5$).[16,17]

**NMR Spectroscopy.** All experiments were recorded on a Varian INOVA 500 MHz $^1$H NMR spectrometer using a Varian broadband indirect single-axis (z-coil) PFG probe. The sample temperature was calibrated using the chemical shift difference (Δppm) between the two resonances of a neat methanol standard sample to within ±0.1 °C of the desired temperature.[18] One-dimensional $^1$H spectra were used to directly measure the actual $w_0$. All samples were monitored at +20 and −30 °C; however, to add completeness to the study and after the main experimental design, the 1.5 M NaCl sample was evaluated at −40 °C (Figure 5).

Gradient-selected sensitivity-enhanced $^{15}$N HSQC experiments were used to observe resonances that in turn monitor protein structure. The $^{15}$N HSQC experiment is ideal for protein denaturation studies because it monitors resonances of amide groups throughout the protein. Therefore, local and global structural perturbations are detected as either change in chemical shift or complete disappearance of the resonance. The $^{15}$N HSQC experiment has become a standard assay of the folded state of polypeptides.[19−21]

## Results

The structure of human ubiquitin was monitored by $^{15}$N HSQC NMR experiments as a function of temperature and ionic strength. The temperature used in these studies was varied from +20 to −30 °C, and the ionic strength of the samples was modulated by varying concentrations of NaCl. The four samples used in this study were prepared to investigate ionic strength and water loading effects (see Materials and Methods). Samples were initially characterized by $^{15}$N HSQC and $^1$H 1D NMR at +20 °C to verify the sample integrity and monitor the effects of high ionic strength. Low-temperature effects were characterized at −30 °C, again using $^{15}$N HSQC and $^1$H 1D spectra. Finally, at various time intervals and with differing amounts of agitation, the samples were characterized again at +20 °C. The second set of +20 °C experiments was used to establish the reversibility of the temperature effects and to monitor the sample integrity. Integration of the resonances from water and the AOT C1′ methylene protons of a $^1$H 1D experiments is a direct and accurate measurement of water loading, which is the ratio of the resonance intensities and characterizes the molar ratio of water to surfactant.

A comparison of resonances in the $^{15}$N HSQC spectra of encapsulated ubiquitin recorded at +20 °C relative to those in spectra recorded at temperatures at −30 °C reveals both significant changes in chemical shifts and partial or complete loss of intensity. The water loading capacity of the reverse micelles decreased with decreasing temperature, causing exclusive water loss. Previous studies have suggested that exposure to low temperatures leads to coprecipitation of both the reverse micelle aqueous core and the surfactant.[22,23] However, results of our work confirm that relatively and exclusively pure water is lost from the aqueous core of the reverse micelle. The

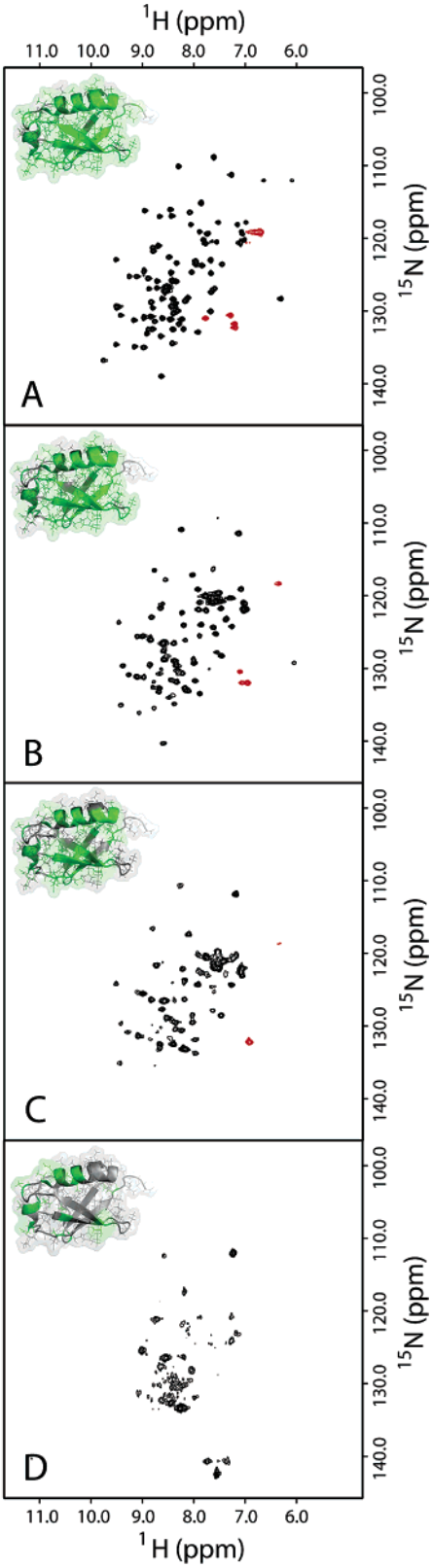


***Figure 5.*** Modulation of reverse micelle−protein interactions by high ionic strength reveals low-temperature two-state unfolding. Panels A−D show $^{15}$N HSQC spectra recorded at 500 MHz ($^1$H) and 100 mM AOT, 50 mM NaOAc, pH 5.0, and 1.5 M NaCl. From (A)−(D), spectra were recorded at +20, −20, −30, and −40 °C. All spectra were recorded and processed under identical conditions − note that spectrum D is displayed at a topographical level ∼50% closer to the noise floor than the other spectra. Observed amide correlations mapped onto a structural model of ubiquitin are highlighted in green.

(16) Lesser, M. E.; Luisi, P. L. *Chimia* **1990**, *44*, 270−282.
(17) Babu, C. R.; Flynn, P. F.; Wand, J. A. *J. Biomol. NMR* **2003**, *25*, 313−323.
(18) Van Geet, A. L. *Anal. Chem.* **1970**, *42*, 679−680.
(19) Kuwajima, K.; Kim, P. S.; Baldwin, R. L. *Biopolymers* **1983**, *22*, 59−67.
(20) McIntosh, L. P.; Griffey, R. H.; Muchmore, D. C.; Nielson, C. P.; Redfield, A. G.; Dahlquist, F. W. *Proc. Natl. Acad. Sci. U.S.A.* **1987**, *84*, 1244−1248.
(21) Roder, H.; Wuthrich, K. *Proteins* **1986**, *1*, 34−42.
(22) Hauser, H.; Haering, G.; Pande, A.; Luisi, P. L. *J. Phys. Chem.* **1989**, *93*, 7869−7876.
(23) Munson, C. A.; Baker, G. A.; Baker, S. N.; Bright, F. V. *Langmuir* **2004**, *20*, 1551−1557.

***Table 1.*** Water Loading Capacity as a Function of Ionic Strength[a]

| ionic strength | $w_0$ at +20 °C | $w_0$ at −30 °C | $\Delta w_0$ |
|---|---|---|---|
| $H_2O$ | 37.6 | 7.0 | 30.6 |
| 0.25 M NaCl | 26.9 | 9.7 | 17.2 |
| 1.0 M NaCl | 27.0 | 13.9 | 13.1 |
| 1.5 M NaCl | 18.9 | 16.0 | 2.9 |

[a] Two trends appear as the ionic strength of the sample is increased. First, at room or meso temperatures, and in the limit of low ionic strength buffers, the water loading of a reverse micelle sample is maximal. The second trend is that water loading capacity at low temperatures increases as ionic strength is increased (these two trends are shown in the second and third columns). The forth column is the difference between water loadings ($\Delta w_0$) at +20 and −30 °C. The apparent disparity between $w_0$ values of the 0.25 and 1.0 M at +20 °C is explained in the Reverse Micelle Sample Preparation subsection of the Materials and Methods section.

conductance of water lost from reverse micelles (without ubiquitin) reconstituted from a 1.5 M NaCl solution and exposed to −20 °C until equilibrium is equivalent to a ∼270 nM NaCl solution, which represents a decrease in the salt concentration of approximately 4 orders of magnitude. We believe that improved phase separation methods will confirm that the water shed at low temperatures is of even higher purity. Water loss from the interior of the reverse micelle limits the solvation available for host molecule encapsulation and can promote low-temperature artifacts. Of particular significance is the fact that the extent of water loss is decreased by increasing ionic strength of the reverse micelle sample.

The water loading capacity at +20 °C is observed to decrease with increasing ionic strength; however, at low temperature, −30 °C, the higher ionic strength actually stabilizes higher water loading (Table 1). Water from the interior of the reverse micelle precipitates or sheds at low temperatures (e.g., −30 °C) and collects in the bottom of the NMR tube as ice. We will subsequently refer to the loss of water content of the reverse micelle particles as water shedding. As water sheds, the radius of the reverse micelle naturally decreases, an effect that has important consequences for the physical state of the encapsulated molecule. Interestingly, the low-temperature effects on ubiquitin and water loading were fully reversible, as confirmed by recovery of the initial water loading when samples were returned to +20 °C and identical $^{15}$N HSQC spectra (Figure 2). Water loading slowly increased (about 1 $w_0$ unit per day) to the original $w_0$ value after cooling and then warming the sample under passive conditions, for example, with no agitation. The process of water uptake can be expedited by sample agitation, and vigorous agitation returns the sample to its original condition within minutes. We also found that water shedding occurs regardless of the presence of ubiquitin (data not shown). The fact that water shedding occurs with or without protein indicates that the increase in ionic strength affects either the structure of the encapsulated water, the surfactant, or both.

Ubiquitin structure was unperturbed by varied ionic strength conditions at +20 °C as evaluated by $^{15}$N HSQC experiments (Figure 3). It is noteworthy, however, that substantial changes in resonances are observed in the $^{15}$N HSQC for all ionic strength spectra at −30 °C relative to the +20 °C spectra. At low ionic strength, spectral features are consistent with a loss of protein structure. The influence of elevated ionic strength increases the number of observed resonances and decreases the line width of $^{15}$N HSQC resonances. This result confirms that ubiquitin retains substantial stability at low temperatures in the presence of higher ionic strength. Nevertheless, even under high ionic strength and concomitantly higher levels of hydration, a number of resonances are shifted or missing. The ubiquitin models in Figure 4 show the differences in observed resonances, highlighted in green, between the low ionic strength and high ionic strength samples (spectra A and D). The main difference between the detected resonances of these two samples is that under low ionic strength conditions only a single face of the protein has detectible resonances, whereas in the limit of high ionic strength, resonances from the entire protein are observed. This result suggests that ionic strength can be used to distinguish between two effects that influence protein structure and are detected at low temperature, reverse micelle−protein interactions and cold denaturation.

## Discussion

Studies of protein structure and dynamics conducted at low temperature represent a new direction in biophysics, and such studies are anticipated to yield important insights into stability, folding pathways, and folding intermediates of proteins. Our results demonstrate that high-resolution protein NMR studies can be conducted at low temperature. Interpreting low-temperature data, however, especially distinguishing between protein−reverse micelle interactions and low-temperature effects (e.g., cold denaturation), is subtle. On the other hand, our data demonstrate that we have complete experimental control over the interaction between the protein surface and the headgroups of the surfactant, which allows us to directly observe cold denaturation. As a component of our results, we describe a new reverse micelle physical phenomenon called water shedding and discuss how water shedding impacts low-temperature studies of encapsulated biomacromolecules.

A general complication of all cold denaturation studies is the unambiguous attribution of observations to cold denaturation effects as opposed to other influences.[12] For example, a standard vehicle for raising protein cold denaturation temperature above 0 °C is the common use of either denaturants or applied elevated external pressure to destabilize the protein under investigation.[12,24] These strategies arise out of the practical difficulty of studying proteins below the freezing point of water, for example, in the solid state. Reverse micelles provide an effective alternative approach to studies of cold denaturation, allowing examination of protein stability down to at least −40 °C.

**Characterization of Water Shedding.** Water loading ($w_0$) can be varied over a wide range for AOT reverse micelles, with typical water loadings ranging from 1 to about 60 for the sodium salt of AOT.[23,25,26] The measured water loading not only provides information about the relative amount of water to surfactant, but also reflects the reverse micelle size and amount of water available for host molecule solvation. Water loading values for the reverse micelle samples prepared with increasing added salt concentrations at the various temperatures are presented in Table 1.

Water loading is directly and conveniently measured by $^1$H 1D solution NMR. The $^1$H NMR spectrum of AOT has previously been assigned, which allows us to readily identify resonances of unit proton intensity.[27] The C1′ methylene proton

(24) Marques, M. I.; Borreguero, J. M.; Stanley, H. E.; Dokholyan, N. V. *Phys. Rev. Lett.* **2003**, *91*, 138103-1−138103-4.
(25) Luisi, P. L. *Angew. Chem.* **1985**, *24*, 439−450.
(26) Zulauf, M.; Eicke, H.-F. *J. Phys. Chem.* **1979**, *83*, 480−486.
(27) Ueno, M.; Kishimoto, H.; Kyogoku, Y. *Chem. Lett.* **1977**, 599−602.

resonances of AOT are convenient for water loading measurements because they are well separated from the aliphatic surfactant, solvent, and water resonances. The intensities of these resonances relative to the water resonance in a $^1$H 1D spectrum provide an accurate experimental measure of the water loading, which represents a fundamental parameter in the physiochemical studies of encapsulated molecules.

Inasmuch as a low water loading value corresponds to small reverse micelle size, the change in water loading values between two temperatures (e.g., water shedding) also represents a change in the radius of the water−protein core of the reverse micelle as the temperature is altered. We define water shedding as the change in water loading capacity at two temperatures (e.g., $w_{0\text{Temperature1}} - w_{0\text{Temperature2}}$). Exposure of the aqueous nanodispersion to low temperature leads to a phase separation wherein the water inside of the reverse micelle is lost, forming a biphasic system with the bulk solution (AOT and pentane). The water loading capacity at a given temperature depends on the ionic strength of the sample.[28,29] Near room temperature, the water loading capacity of the reverse micelle is inversely proportional to the ionic strength, so that at high ionic strength the amount of water that can be encapsulated decreases. However, the opposite trend occurs for water loading capacity at low temperature, and at −30 °C the samples with high ionic strength have higher water loading values (these opposing trends are shown in Table 1).

The change in water loading ($\Delta w_0$) for the reverse micelle sample prepared with 1.5 M NaCl at +20 and −30 °C is minimal, indicating that the size and physical properties of the reverse micelles under these conditions are virtually identical. Simple calculations of the 1.5 M NaCl reverse micelle sample indicate that there is only a 3.5% decrease in the radius of the reverse micelle at +20 °C relative to the −30 °C particle. For this sample, the change in water loading values corresponds to about 1.3 Å difference in the radius (e.g., the reverse micelle radius is 36.7 Å at +20 °C and 35.4 Å at −30 °C). By comparison, the water sample undergoes a large change in water loading of 30.6 units; such a large difference equates to about 12.9 Å or a 30% change in the radius of the reverse micelle.

**Screening Reverse Micelle−Protein Interactions Supports Detection of Cold Denaturation.** The most direct interpretation of the data presented herein is that as the size of the reverse micelle decreases (as measured by low water loadings), the structure of the encapsulated protein, ubiquitin in the present example, is perturbed by the collapsing electrostatic surface lining the anterior surface of the reverse micelle. In this view, high ionic strength affects the physical properties of the reverse micelle, and ubiquitin can be thought to be a probe of the reverse micelle structure and size. This hypothesis is consistent with our data, suggesting that cold denaturation detection is obscured by reverse micelle−protein interactions at low ionic strengths; however, under appropriately high ionic strength conditions, reverse micelle−protein interactions are screened because the reverse micelle size is larger. The water shedding differences ($\Delta w_0$) between the high ionic strength sample (1.5 M NaCl) and the water sample ($H_2O$) lead to substantial changes at low temperature in ubiquitin. As stated earlier, the size of the reverse micelle particle is proportional to the water loading; moreover, the water loading is also a measure of the amount of water available for ubiquitin solvation. Under low water loading conditions, the amount of water available to solvate or stabilize ubiquitin is diminished. At low temperature and ionic strength, the radius of the reverse micelle is at a minimum, and under these conditions protein−reverse micelle interactions are enhanced, leading to ubiquitin destabilization.

This change in the reverse micelle size (based on the $\Delta w_0$) is minimized by high ionic strength, and as a result ubiquitin is more stable at −30 °C for the 1.5 M NaCl sample than at lower ionic strengths (see Figure 4).[30] We attribute the relationship between the ionic strength and ubiquitin stability to the size ($w_0$) of the reverse micelle, which is confirmed by direct measurement of the water loading. As ionic strength is increased, water loss is decreased, which supports the stabilization of larger reverse micelles at low temperature. A reduction in the water available for protein solubilization and screening of the electronic double layer leads to destabilization of ubiquitin structure. The larger reverse micelle minimizes the protein−reverse micelle interactions, which allows for detection of cold denaturation (Figure 5).

The low water loading differences of reverse micelles reconstituted from solutions of high ionic strength at +20 and −30 °C indicate that the size and shielding influences effectively modulate the experimentally detected denaturing effects between reverse micelle−protein interactions and cold denaturation. Under these conditions, changes in chemical shifts as well as loss of HSQC resonances as the temperature is decreased from +20 and −30 °C of the 1.5 M NaCl sample can be attributed to cold denaturation of ubiquitin. Changes in the chemical shift of resonances in an HSQC spectrum indicate a change in local electronic environment experienced by a given nucleus, and the complete disappearance of resonances in an HSQC spectrum is caused by exchange between multiple environments and most commonly attributed to a loss of unique structure. The fact that there is minimal change in water loading and hence size between +20 and −30 °C HSQC spectra of the 1.5 M NaCl sample indicates that there are structural changes in ubiquitin that arise primarily from the low-temperature cold denaturation. Coupling the observation that the 1.5 M NaCl reverse micelles are larger with the fact that the $^{15}$N HSQC spectrum at this ionic strength has the best proton dimension dispersion suggests that reverse micelle−protein interactions dominate denaturation at low ionic strengths, but can be effectively screened to allow direct observation of cold denaturation using high ionic strength buffer (Figure 4).

The ionic strengths of the reconstitution buffers used in this study were carefully chosen to bracket the standard 0.25 M NaCl, which is commonly employed for use in reverse micelle protein encapsulation studies.[8] At +20 °C, the $^{15}$N HSQC spectra recorded for ubiquitin reconstituted in the various conditions are virtually identical, indicating that ubiquitin is properly and uniquely folded at all ionic strengths (at +20 °C, see Figure 3). It is worth mentioning that the general intensity of the 1.5 M NaCl sample HSQC spectrum is somewhat diminished as compared to the other samples. The decrease in resonance intensity reflects lower encapsulation efficiency at high ionic strength. Protein encapsulation efficiency decreases at high ionic strength and low water loadings.[16,17]

(28) Kon-No, K.; Kitahara, A. *J. Colloid Interface Sci.* **1971**, *41*, 47−51.
(29) Kon-No, K.; Kitahara, A. *J. Colloid Interface Sci.* **1970**, *33*, 124−132.
(30) Hou, M. J.; Shah, D. O. *Langmuir* **1987**, *3*, 1086−1096.

**Water Shedding by Reverse Micelles Can Be Used To Investigate Protein Confinement.** As water is lost from the reverse micelle core to the surroundings, the reverse micelle becomes smaller, an effect that suggests that reverse micelles should be useful for investigating proteins under a variety of confining, desolvating, and electrostatic environments. By varying the ionic strength buffer of a reverse micelle sample and/or the temperature, to conditions that promote water shedding, proteins can be studied under a continuum of conditions.

Water shedding is a reversible process, and the water shed at low temperature is re-encapsulated after the system is returned to room temperature. The uptake of water at room temperature after shedding is approximately one water loading ($w_0$) unit per day, which is slow enough to target a specific $w_0$ value and monitor the influence on the protein. One could thus use the process of water shedding and uptake as a way to fine-tune the water loading by separating the water phase from the pentane−reverse micelle phase when the desired water loading is attained. The biphasic system that forms from water shedding is maintained at room temperature with slow water uptake, which lends to precise control of the water loading and thus the degree of confinement. The initial water loading can be restored quickly by sample agitation. The technique of temperature-driven water shedding (at low temperatures) and the subsequent water uptake (at room temperatures) show great promise for studying the influence of confinement and solvation on molecular structure.

**Ubiquitin Cold Denaturation.** Ubiquitin is known to have a promiscuous binding face that interacts with many different protein domains. Among the known ubiquitin binding domains are UBAs (ubiquitin associated domains), UIMs (ubiquitin interacting motifs), CUE (coupling of ubiquitin to ER degradation), and NZFs (Nlp14 zinc fingers).[31−35] Ubiquitin interacts with binding partners along what is known as the I44 surface, which is composed of a small patch of hydrophobic residues surrounded by a group of basic residues.[36,37] The electrostatic surface map of ubiquitin reveals that the protein can be roughly split into two electrostatic regions (see Figure 6). The I44 surface of ubiquitin is predominantly electropositive and hydrophobic, whereas the potential on the opposite surface is electronegative (Figure 6). Ubiquitin $^{15}$N HSQC experiments conducted under low ionic strength and low temperature conditions probe regions of the protein that are more sensitive to the reverse micelle−protein interactions as well as the nature of the cold denaturation (e.g., local or global). In the limit of low ionic strength and low temperature, reverse micelle−protein interactions dominate low-temperature effects.[38] Resonances corresponding to residues that make up the I44 face are lost at low temperature and low ionic strength; however, under the same conditions we observe resonances that are associated with the opposed electronegative face. This indicates that the I44 surface is most affected by the electrostatic interaction with the anionic headgroups of the reverse micelle surfactants, whereas the electronegative face is relatively unperturbed. This differential perturbation is caused by the interaction of the ubiquitin binding face with the negatively charged anterior surface of the reverse micelle.

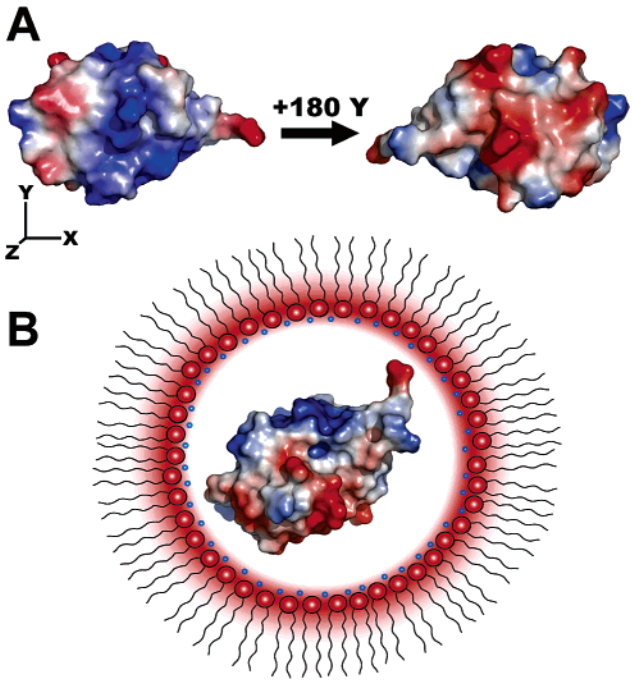


***Figure 6.*** (A) Electrostatic surface of ubiquitin. As ubiquitin is rotated 180° along the *Y*-axis, the general electrostatic surface potential changes sign. The blue is electropositive, and the red is electronegative. Near the bottom of the electropositive half of ubiquitin (as shown) is the I44 surface. Under low ionic strength conditions, $^{15}$N HSQC resonances corresponding to the electropositive half of the protein are not detected. However, under high ionic strength conditions, resonances from all portions of ubiquitin are detected (although many resonances disappear or shift). (B) A schematized reverse micelle showing general electrostatics of the reverse micelle and the protein. The blue spheres correspond to positively charged sodium counterions, which are relatively small and mobile. The basic portion of the protein (blue) undergoes conformational exchange driven by an electrostatic interaction with the anterior surface of the reverse micelle (generally red). Reverse micelle and ubiquitin are not to precise scale.

Importantly, we detect resonances at high ionic strength and low temperature that correspond to residues from throughout the protein. In the limit of high ionic strength and low temperature, reverse micelle−protein interactions are eliminated and cold denaturation effects are detected. The observation of cold denaturation in ubiquitin is subtle due to the high thermodynamic stability of this protein. However, our data show a general collapse in the proton dimension and loss of resonance intensity from residues throughout the protein, consistent with a simple two-state unfolding mechanism.[39−42]

A previous low-temperature study of encapsulated ubiquitin indicates that cold denaturation is exclusively seen along the I44 surface, indicating that ubiquitin is cold denatured in a globally noncooperative manner.[38] We note that in the previous

(31) Fisher, R. D.; Wang, B.; Alam, S. L.; Higginson, D. S.; Robinson, H.; Sundquist, W. I.; Hill, C. P. *J. Biol. Chem.* **2003**, *278*, 28976−28984.
(32) Ponting, C. P. *Biochem. J.* **2000**, *351*, 527−535.
(33) Alam, S. L.; Sun, J.; Payne, M.; Welch, B. D.; Blake, B. K.; Davis, D. R.; Meyer, H. H.; Emr, S. D.; Sundquist, W. I. *EMBO J.* **2004**, *23*, 1411−1421.
(34) Wang, Q.; Goh, A. M.; Howley, P. M.; Walters, K. J. *Biochemistry* **2003**, *42*, 13529−13535.
(35) Wang, B.; Alam, S. L.; Meyer, H. H.; Payne, M.; Stemmler, T. L.; Davis, D. R.; Sundquist, W. I. *J. Biol. Chem.* **2003**, *278*, 20225−20234.
(36) Beal, R.; Deveraux, Q.; Xia, G.; Rechsteiner, M.; Pickart, C. *Proc. Natl. Acad. Sci. U.S.A.* **1996**, *93*, 861−866.
(37) Verma, R.; Peters, N. R.; D'Onofrio, M.; Tochtrop, G. P.; Sakamoto, K. M.; Varadan, R.; Zhang, M.; Coffino, P.; Fushman, D.; Deshaies, R. J.; King, R. W. *Science* **2004**, *306*, 117−120.
(38) Babu, C. R.; Hilser, V. J.; Wand, A. J. *Nat. Struct. Mol. Biol.* **2004**, *11*, 352−357.
(39) Brandts, J. F. *J. Am. Chem. Soc.* **1964**, *86*, 4291−4301.
(40) Tanford, C. *Adv. Protein Chem.* **1968**, *23*, 121−282.
(41) Tanford, C. *Adv. Protein Chem.* **1970**, *24*, 1−95.
(42) Shellman, J. A. *Biophys. Chem.* **2002**, *96*, 91−101.

study, relatively low ionic strength encapsulation buffer was used, and in this situation the reverse micelles are particularly vulnerable to loss of water at low temperature, resulting in reverse micelle−protein interactions between the I44 surface and the oppositely charged reverse micelle surface. In the limit of low ionic strength, reverse micelle−protein interactions obscure the nature of the low-temperature unfolding, whereas under conditions that promote cold denaturation detection ubiquitin appears to unfold via a two-state mechanism.

Chemical shift dispersion of amide proton resonances is commonly taken to be an accurate assay of the folded state of the protein. Our amide proton chemical shift dispersion results agree with other published studies of unfolded ubiquitin, which confirm that the residual dispersion present in the unfolded state depends on the type of denaturant (e.g., chemical versus pressure denaturation) and the relative protein populations of folded versus unfolded forms.[43−46]

## Conclusions

The combination of reverse micelle supported encapsulation and solution NMR spectroscopy provides a powerful tool for the investigation of the physical properties of biomacromolecules at low temperatures. A new method for accessing the cold denatured state of ubiquitin was developed by increasing the ionic strength of the reverse micelle reconstitution buffer, which screens reverse micelle−protein interactions that otherwise interfere with observations of cold denaturation. Water shedding, a new reverse micelle phenomenon, is reported and characterized as the difference of water loading values ($\Delta w_0$) between two temperatures for a given sample. Samples reconstituted with low ionic strength that are subject to low-temperature shed water to form a biphasic system with the reverse micelle solution.

The process of protein encapsulation is simple and well established, and investigating encapsulated proteins at low temperatures is an obvious extension of reverse micelle studies. However, when investigating encapsulated protein cold denaturation, it is imperative to appreciate the effects of water shedding and potential artifacts that can mask cold denaturation, such as reverse micelle−protein interactions. The data and methods of the current study provide an improved set of procedures for the general investigation of encapsulated proteins at low temperature or in other extreme conditions.

**Acknowledgment.** We acknowledge the support of a Seed Grant Award from the University of Utah Research Foundation. A.K.S. is supported by an NIH training grant (GM8537).

JA052805I

(43) Harding, M. M.; Williams, D. H.; Woolfson, D. N. *Biochemistry* **1991**, *30*, 3120−3128.
(44) Schick, M.; Bruschweiler, B.; Ernst, R. R. In *High-pressure research in the biosciences and biotechnology*; Heremans, K., Ed.; Leuven University Press: Leuven, 1997; pp 27−30.
(45) Brutscher, B.; Bruschweiler, R.; Ernst, R. R. *Biochemistry* **1997**, *36*, 13043−13053.
(46) Peti, W.; Smith, L. J.; Redfield, C.; Schwalbe, H. *J. Biomol. NMR* **2001**, *19*, 153−165.